Kinetics of Thermal Decomposition of Cubic Ammonium Perchlorate

Sergey Vyazovkin and Charles A. Wight*

Center for Thermal Analysis, Department of Chemistry, University of Utah, 315 S., 1400 E., Salt Lake City, Utah 84112

Received July 13, 1999. Revised Manuscript Received September 7, 1999

The methods of thermogravimetric analysis (TGA) and differential scanning calorimettry (DSC) have been used to study the thermal decomposition of ammonium perchlorate (AP). TGA curves obtained under both isothermal and nonisothermal conditions show a characteristic slowdown at the extents of conversion, $\alpha = 0.30-0.35$. DSC demonstrates that in this region the process changes from an exothermic to an endothermic regime. The latter is ascribed to dissociative sublimation of AP. A new computational technique (advanced isoconversional method) has been used to determine the dependence of the effective activation energy (E_α) on α for isothermal and nonisothermal TGA data. At $\alpha > 0.1$, the E_α dependencies obtained from isothermal and nonisothermal data are similar. By the completion of decomposition ($\alpha \rightarrow 1$) the activation energy for the isothermal and nonisothermal decomposition respectively rises to ∼110 and ∼130 kJ mol^{-1}, which are assigned to the activation energy of sublimation. The initial decomposition ($\alpha \rightarrow 0$) shows the activation energy of 90 kJ mol^{-1} for the isothermal decomposition and 130 kJ mol^{-1} for the nonisothermal decomposition. The difference is explained by different rate-limiting steps, which are nucleation and nuclei growth for isothermal and nonisothermal decompositions, respectively.

Introduction

As a key energetic material for rocket technologies, ammonium perchlorate (AP) continues to inspire new and new research efforts[1−6] to better understand its thermal decomposition. A significant amount of information on the process had been produced by the 1970s and is covered in several reviews.[7−10] Among many peculiar features, the most striking was the discovery of low- and high-temperature modes of decomposition. The low-temperature decomposition (LTD) occurs below approximately 300 °C and results only in ∼30% decomposition. The high-temperature decomposition (HTD) is observed above 300 °C and leads to complete gassification of AP. At 240 °C, AP undergoes a transition from orthorhombic to cubic crystalline form. The practical interest is primarily focused on the thermal decomposition of cubic AP. The kinetics of this process has been the subject of many studies.[1,3,6,11−30] Some of the results of these studies are collected in Tables 1 and 2. The reported effective activation energies vary from ∼37 to 260 kJ mol^{-1}. The interpretation of the values is also different. The confusing character of the kinetic information is not very surprising, for the process is known[7−10]

(1) Brill, T. B.; Brush, P. J.; Patil, D. G. *Combust. Flame* **1993**, *94*, 70.
(2) Yoo, M.; Yoon, S.; De Lozanne, A. *J. Vac. Sci. Technol. B*, **1994**, *12*, 1638.
(3) Oxley, J. C.; Smith, J. L.; Valenzuela, B. R. *J. Energ. Mater.* **1995**, *13*, 57.
(4) Sharma, J.; Coffey, C. S.; Ramaswamy, A. L.; Armstromg, R. W. *Mater. Res. Soc. Symp. Proc.* **1996**, *418*, 257.
(5) Ramaswamy, A. L.; Shin, H.; Armstromg, R. W.; Lee, C. H.; Sharma, J. *J. Mater. Sci.* **1996**, *31*, 6035.
(6) Ganga Devi, T.; Kannan, M. P.; Hema, B. *Thermochim. Acta* **1996**, *285*, 269.
(7) Jacobs, P. W. M.; Whitehead, H. M. *Chem. Rev.* **1969**, *69*, 551.
(8) Keenan, A. G.; Siegmund, R. F. *Quart. Rev. Chem. Soc.* **1969**, *23*, 4303.
(9) Pearson, G. S. *Oxid. Combust. Rev.* **1969**, *4*, 1.
(10) Solymosi, F. *Structure and Stability of Salts of Halogen Oxyacids in the Solid Phase*; J. Wiley & Sons: London, 1977; p 195.
(11) Bircumshaw, L. L.; Newman, B. H. *Proc. R. Soc. (London)* **1954,** *A227*, 115.
(12) Bircumshaw, L. L.; Newman, B. H. *Proc. R. Soc. (London)* **1955**, *A227*, 228.
(13) Bircumshaw, L. L.; Phillips, T. R. *J. Chem. Soc.* **1957**, 4741.
(14) Galwey, A. K.; Jacobs, P. W. M. *J. Chem. Soc.* **1959**, 837.
(15) Galwey, A. K.; Jacobs, P. W. M. *Proc. R. Soc. (London)* **1960**, *A254*, 455.
(16) Raevskii, A. B.; Manelis, G. B. *Dokl. Akad. Nauk SSSR* **1963**, *151*, 886.
(17) Solymosi, F.; Revesz, L. *Kinet. Katal.* **1963**, *4*, 88.
(18) Shidlovskii, A. A.; Shmagin, L. F.; Bulanova, V. V. *Izvest. Vyssh. Uchebn. Zaved., Khim. Khim. Tekhnol.* **1965**, *8*, 533.
(19) Manelis, G. B.; Rubtsov, Yu. I. *Russ. J. Phys. Chem.* **1966**, *40*, 416.
(20) Inami, H. S.; Rosser, W. A.; Wise, H. *Trans. Faraday Soc.* **1966**, *62*, 723.
(21) Davies, J. V.; Jacobs, P. W. M.; Russel-Jones, A. *Trans. Faraday Soc.* **1967**, *63*, 1737.
(22) Maycock, J. N.; Pai Verneker, V. R. *Proc. R. Soc. (London)* **1968**, *A307*, 303.
(23) Jacobs, P. W. M.; Russel-Jones, A. *J. Phys. Chem.* **1968**, *72*, 202.
(24) Aleksandrov, V. V.; Gladkikh, V. M.; Khlevnoi, S. S. *Combust., Explosion, Shock Waves* **1969**, *5*, 400.
(25) Boldyrev, V. V.; Alexandrov, V. V.; Boldyreva, A. V.; Gristan, V. I., Karpenko, Yu. Ya.; Korobeinitchev, O. P.; Panfilov, V. N.; Khairetdinov, E. F. *Combust. Flame* **1970**, *15*, 71.
(26) Pai Verneker, V. R.; McCarty, M.; Maycock, J. N. *Thermochim. Acta* **1971**, *3*, 37.
(27) Jacobs, P. W. M.; Ng, W. L. J. *Solid State Chem.* **1974**, *9*, 315.
(28) Morisaki, S.; Komamiya, K. *Thermochim. Acta* **1975**, *12*, 239.
(29) Kishore, K.; Pai Verneker, V. R.; Krishna Mohan, V. *Thermochim. Acta* **1975**, *13*, 277.
(30) Tompa, A. S. *Thermochim. Acta* **1984**, *77*, 133.

10.1021/cm9904382 CCC: $18.00
Published on Web 10/27/1999

Table 1. Activation Energies for Thermal Decomposition of Ammonium Perchlorate under Ambient and Subambient Pressures

measurement	P, atm	T region, °C	conversion	kinetic eq	E, kJ mol^{-1}	ref
pressure vs time, isothermal	0.53, N_2	380−440	complete	original AP:		14
				α^n, $\alpha = 0.26-0.92$	73.2	
				$1-(1-\alpha)^{1/3}$	162.2	
				$\alpha = 0-0.7$		
			∼30−100%	LTD residue:		
				α^n, $\alpha = 0.15-0.40$	125.4	
				α^n, $\alpha = 0.43-0.95$	125.4	
microscopic, isothermal	1, air	250−272			71.1	16
volume vs time, isothermal	1, air	249−267	∼30%	$-[\ln(1-\alpha)]^{1/3}$	132.1	17
				$\alpha = 0.05-0.5$		
mass vs time, isothermal	1, air	250−300	∼30%	$-[\ln(1-\alpha)]^n$		18
				$\alpha = 0-0.2$	104.9	
		330−450	∼25−100%	LTD residue:		
				$-[\ln(1-\alpha)]^n$		
				$\alpha = 0-0.4$	163.4	
				$\alpha = 0.55-0.85$	148.4	
mass vs time, isothermal,	1, air	245−280	∼30%	$k_1(1-\alpha)^2 + k_2\alpha(1-\alpha)^2$	$E_1 = 125.4$	19
					$E_2 = 75.7$	
dT/dt vs T, adiabatic	1, air	250−325	∼30%	$-\ln(1-\alpha)$, $T > 300$	130.0	20
pressure vs time, isothermal	0.96, air	240−280	∼30%	$[-\ln(1-\alpha)]^{1/2}$	112.7	21
				$\alpha = 0.03-0.85$		
mass vs time, isothermal	1, air	210−360	30−100%	LTD residue:		
				$1-(1-\alpha)^{1/3}$	117.2	
pressure vs time isothermal	0.53	200−250	∼30%	$\log(t_{0.8} - t_{0.2})$ vs T^{-1}	125.4	22
		250−350	complete		83.0	
		370−440	complete		189.8	
mass vs time, isothermal	1, air	304−375	∼30−100%	LTD residue:		23
				$1-(1-\alpha)^{1/2}$	127.9	
mass vs T, nonisothermal	1, air	315−385	complete	α = const		26
				315−330	125.4	
				330−360	83.6	
				360−380	188.1	
pressure vs t, isothermal		220−290	complete	$-\ln(1-\alpha)$		27
				nucleation	85.3	
				nuclei growth	115.0	
mass vs T, nonisothermal	1, He	240−420	complete	$\ln\beta$ vs $1/T_\alpha$		28
				$\alpha > 0.4$	98.7	
heat flow vs T, nonisothermal	1, pierced pan	240−480	complete	$\ln(d\alpha/dt)$ vs $1/T_\alpha$		29
			2 exo peaks	1st exo:		
				$\alpha = 0.2$	92.4	
				$\alpha = 0.5$	92.4	
				$\alpha = 0.8$	98.7	
				2nd exo:		
				$\alpha = 0.5$	261.3	
				$\alpha = 0.8$	245.4	
heat flow vs T, isothermal	1, pierced pan	268−303	∼28%, exo peak	$\ln(d\alpha/dt)$ vs $1/T_\alpha$		29
				$\alpha = 0.2$	73.6	
				$\alpha = 0.5$	96.1	
				$\alpha = 0.8$	96.1	
mass vs T, nonisothermal, 1.5 10^4 C min^{-1}	1	>300	complete	$(1-\alpha)^n$, $\alpha < 0.5$	37.6	1
heat flow vs T, nonisothermal	sealed glass tube	250−400	complete	$\ln(\beta/T^2_m)$ vs $1/T_m$	95	3
$[NH_4^+]$ vs t isothermal, ion chromatography	sealed glass tube	235−385		$-\ln(1-\alpha)$, $\alpha < 0.7$	85	3
mass vs t, isothermal	1, air	260−270	∼30%	$-\ln(1-\alpha)$, $\alpha < 0.5$	141.2	6

to be a tangled interplay of various chemical (solid-state decomposition, reaction of gaseous products with the solid, gas-phase reactions) and physical (polymorphic transition, diffusion, sublimation, adsorption−desorption) phenomena. The effective activation energy of the thermal decomposition of AP is obviously a composite value determined by the activation energies of elementary steps as well as by the relative contributions of these steps to the overall reaction rate. Because the ratio of these contributions is determined by the experimental conditions, the effective activation energy tends to show a dependence on experimental parameters, e.g., pressure (cf., Tables 1 and 2).

If a multistep process involves steps with different activation energies, the relative contributions of these steps into the overall reaction rate will vary with both the temperature and extent of conversion. This means that the effective activation energy will also be a

Table 2. Activation Energies for Thermal Decomposition (Dissociative Sublimation) of Ammonium Perchlorate in Vacuum

measurement	*P*, atm	*T* region, °C	conversion	kinetic eq	*E*, kJ mol^{-1}	ref
pressure vs time, isothermal	vacuum	240−275	∼30%	acceleratory:		12
				$\log(t_{0.1})$ vs T^{-1}	76.9	
				$\log(t_{0.5})$ vs T^{-1}	71.5	
				$\ln[\alpha/(1-\alpha)]$	96.1	
				deceleratory:		
				$-\ln(1-\alpha)$	85.6	
				$\ln[\alpha/(1-\alpha)]$	73.2	
pressure vs time, isothermal	vacuum	245−340	∼30%	$-[\ln(1-\alpha)]^{1/2}$ $\alpha = 0.15-0.85$	102.4	15
				acceleratory:		
				$-[\ln(1-\alpha)]^{1/2}$	104.5	
				deceleratory:		
				$\ln[\alpha/(1-\alpha)]$	79.4	
heat flow vs *T*, nonisothermal	6.6×10^{-5} 6.6×10^{-4}	290−410	complete	$\log q$ vs T^{-1} q is initial rate	90.3	24
mass vs *T*, nonisothermal	1.3×10^{-7}	300−385	complete	$f(\alpha) = 1$	83.6	26
mass vs time, isothermal	vacuum	220−380	not reported	$1-(1-\alpha)^{1/3}$ $\alpha = 0-0.93$	77.8	
				$1-(1-\alpha)^{1/2}$ $\alpha = 0-0.96$	69.0	
heat flow vs *T*, nonisothermal	6.6×10^{-3}	220−340	complete	$\ln \beta$ vs T_m^{-1}	88.6	30
mass vs *T*, nonisothermal	6.6×10^{-3}	270−380	complete	$\ln \beta$ vs T^{-1}	92.0	
mass vs time, isothermal	vacuum	290−380	∼30−100%	LTD residue: $1-(1-\alpha)^{1/3}$ $\alpha = 0-0.9$	125.4	23

function of these two variables. For this reason a solid-state decomposition cannot be generally described by a single constant activation energy.[31] Unfortunately, the earlier kinetic evaluations did not make the allowance for possible variations in the activation energy of the thermal decomposition of AP. The activation energies were estimated in terms of single-step kinetics, i.e., under the assumption of the constancy of the activation energy throughout a wide region of the temperatures and the extents of conversion. Therefore, the values obtained in such a way are in fact averages that are rather insensitive to the changes in the mechanism and kinetics with the temperature and the extent of conversion.[31,32]

The isoconversional methods[33−35] of kinetic analysis allow one to reveal a dependence of the activation energy on the extent of conversion and/or on the temperature. The analysis of such a dependence is usually very helpful in drawing mechanistic conclusions about the process.[31,36] In this study, we employ a new computational technique[37] called the "advanced isoconversional method" to explore the multistep kinetics of the thermal decomposition of cubic AP. The main purpose of this work is to reveal the variation of the effective activation energy on the extent of AP conversion and to suggest its rational mechanistic interpretation.

Experimental Section

AP of 99.8% purity (Aldrich) was used as supplied with no further purification. The differential scanning calorimetry (DSC) experiments were performed using a TA Instruments DSC-2910 apparatus. Samples of AP (2−3 mg) were studied in both open and closed (pierced) aluminum pans. The thermogravimetric analysis (TGA) experiments were carried out using a Rheometrics Model 1000M TGA instrument. To reduce thermal gradients and exothermic self-heating, the experiments were performed on small (∼1 mg) samples. The sample temperature, which is controlled by a thermocouple, did not exhibit any significant systematic deviations from the preset linear temperature programs. This observation is consistent with the earlier temperature measurements[38] conducted with a thermocouple directly embedded in a 45-mg sample of AP that showed a maximum temperature deviation of ∼1 °C. Samples of AP were placed in aluminum pans and heated in a flowing atmosphere of nitrogen (100 mL min^{-1}). For experiments carried out under nonisothermal conditions, the instrument was programmed to heat the sample from room temperature at constant heating rates of 5, 7.5, 10, 12.5, and 15 °C min^{-1}. After an initial period of nonlinear heating (<5 min), the programmed linear heating rates were established. The sample temperature versus time curves were used to evaluate the actual heating rates for the temperature region of AP decomposition. The values were estimated to be 5.2, 7.6, 10.5, 12.8, and 15.5 °C min^{-1}.

Isothermal experiments were conducted at the temperatures 265, 270, 275, 280, and 285 °C. For isothermal experiments, the temperature program was optimized to reach the preset isothermal temperature within 1.5 min without overshooting. During the next 1.5 min, the sample temperature was regulated to within ±1 °C of the set point. For the remainder of each run, the sample temperature was maintained within ±0.05 °C.

Results

DSC and TGA. At 240 °C DSC traces (Figure 1) show an endothermic peak corresponding to the transformation of AP from the orthorhombic to cubic form. It is immediately followed by an exothermic effect due to the thermal decomposition. As seen from DSC data, the thermal behavior of AP is markedly different in open

(31) Vyazovkin, S.; Wight, C. A. *Annu. Rev. Phys. Chem.* **1997**, *48*, 125.
(32) Vyazovkin, S.; Wight, C. A. *J. Phys. Chem. A* **1997**, *101*, 8279.
(33) Friedman, H. *J. Polym. Sci.* **1963**, *6C*, 183.
(34) Ozawa, T. *Bull. Chem. Soc. Jpn.* **1965**, *38*, 1881.
(35) Flynn, J. H.; Wall, L. A. *J. Res. Nat. Bur. Stand.* **1966**, *70A*, 487.
(36) Vyazovkin, S. *Int. J. Chem. Kinet.* **1996**, *28*, 95.
(37) Vyazovkin, S. *J. Comput. Chem.* **1997**, *18*, 393.
(38) Jacobs, P. W. M.; Kureishy, A. R. T. *J. Chem. Soc.* **1962**, *556*.

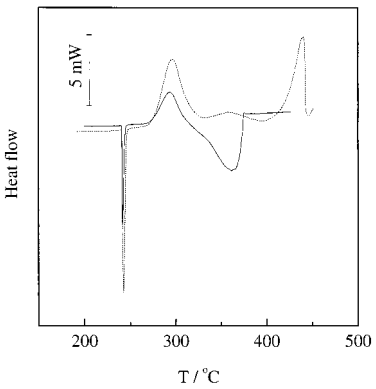

Figure 1. DSC traces of heating AP at a rate of 5 °C min^{-1} in open (solid line) and pierced (dash line) pans. Sample mass is 2.1 and 3.1 mg for the open and pierced pan experiments, respectively.

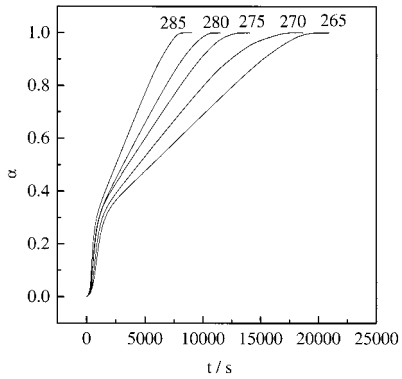

Figure 2. TGA data showing the extent of AP conversion during isothermal decomposition. The temperature of an experiment (in °C) is indicated by each curve.

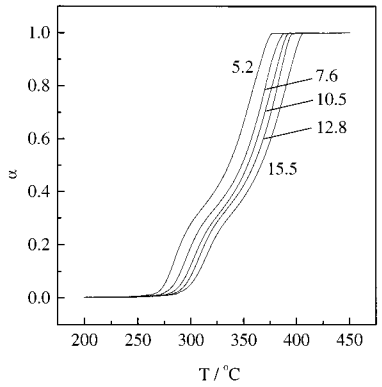

Figure 3. TGA data showing the extent of AP conversion during nonisothermal decomposition. The heating rate of an experiment (in °C min^{-1}) is indicated by each curve.

and closed pans. In a closed pan, the thermal decomposition of AP is completely exothermic. In an open pan, the exothermic decomposition is followed by an endothermic process in the temperature region 310−375 °C (Figure 1).

The results of the isothermal and nonisothermal TGA experiments are respectively shown in Figures 2 and 3. All the TGA curves (Figures 2 and 3) show a slowdown at ∼35% of decomposition which is the salient feature of the process. The isothermal TGA curves show a noticeable induction period (Figure 2). As seen in Figure 3, the nonisothermal decomposition of AP occurs at temperatures above 240 °C, i.e., when AP is in its cubic form.

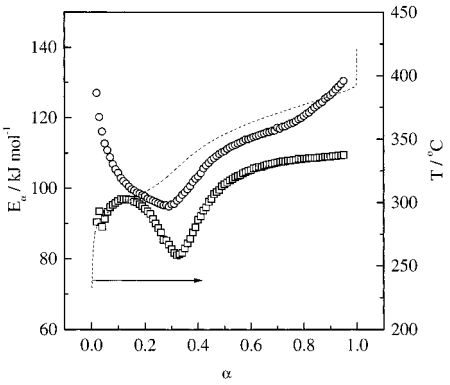

Figure 4. Dependencies of the activation energy on the extent of conversion determined by the isoconversional method for the isothermal (squares) and nonisothermal (circles) TGA data. The *T* vs α curve (dash line) is given to visualize the variation of *E* with *T* for nonisothermal data at an average heating rate 10.5 °C min^{-1}.

Kinetic Computations. The kinetics of solid-state decompositions are customarily described by the basic kinetic equation[39]

$$\frac{d\alpha}{dt} = A \exp\left(\frac{-E}{RT}\right) f(\alpha) \qquad (1)$$

where *A* (preexponential factor) and *E* (the activation energy) are Arrhenius parameters, α is the extent of conversion, $f(\alpha)$ is the reaction model, *t* is the time, *T* is the temperature, and *R* is the gas constant. Vyazovkin developed an advanced isoconversional method,[37] which is based on the assumption that the reaction model is independent of the heating program, *T(t)*. According to this method, for a set of *n* experiments carried out at different heating programs, the activation energy is determined at any particular value of α by finding the value of E_α that minimizes the function

$$\Phi(E_\alpha) = \sum_{i=1}^{n} \sum_{j \neq i}^{n} \frac{J[E_\alpha, T_i(t_\alpha)]}{J[E_\alpha, T_j(t_\alpha)]} \qquad (2)$$

Henceforth, the subscript α denotes the values related to a given extent of conversion. In eq 2, the integral

$$J[E_\alpha, T_i(t_\alpha)] \equiv \int_0^{t_\alpha} \exp\left[\frac{-E_\alpha}{RT_i(t)}\right] dt \qquad (3)$$

is evaluated numerically for a set of experimentally recorded heating program, $T_i(t)$. The minimization procedure is repeated for each value of α to find the dependence of the activation energy on the extent of conversion. An advantage of the advanced isoconversional method is that it uses the actual sample temperature measurements. This makes it possible to account for uncontrollable temperature variations such as those that occur during the initial temperature jump in an isothermal experiment and/or those that result from self-heating/cooling.[37]

The E_α-dependencies evaluated by the isothermal and nonisothermal TGA data are depicted in Figure 4. The E_α-dependence derived from the noniosthermal experi-

(39) Galwey, A. K.; Brown, M. E. *Thermal Decomposition of Ionic Solids;* Elsevier: Amsterdam, 1999.

Table 3. Thermal Events Observed in DTA/DSC Experiments on Thermal Decomposition of Ammonium Perchlorate

thermal events	pan type	atmosphere	pressure, atm	ref
exo/endo		static, vacuum	1.3×10^{-5}	40
exo/exo		static, N_2	1	
exo/exo		static, N_2	4	
0/exo		static, NH_3	4	
exo/exo	Pt	He flow, 17 mL min^{-1}	1	22
exo/endo	Al	static, He, N_2, O_2	1	27
exo/exo		static, He, N_2, O_2	4−51	
exo/exo		static, He	1	
exo/exo		static, He	4−51	
exo/exo	Al, pierced		1	29
exo/exo	Pt	static, air	1	41
exo/endo	Pt	continuous pumping		
exo/endo	Pt	static, vacuum	6.6×10^{-5}	42
exo/exo	pierced	N_2, air	1	30
single exo	sealed			
single endo	pierced	static, vacuum	6.6×10^{-3}	
exo/exo	sealed			3
exo/endo		static, air	1	43
exo/endo	Al, open	N_2 flow, 100 mL min^{-1}	1	present work
exo/exo	Al, pierced	N_2 flow, 100 mL min^{-1}	1	

ment demonstrates two distinct stages in the thermal decomposition of AP. The first stage ($\alpha < 0.3$) is related to the exothermic process. This stage is characterized by a decrease in the activation energy from ∼130 to 95 kJ mol^{-1}. The second stage ($\alpha > 0.3$) corresponds to the endothermic process that shows an increase in the activation energy from 95 to ∼130 kJ mol^{-1}. The E_α-dependence evaluated by the isothermal data can be conventionally divided into three stages: at the first stage ($\alpha < 0.1$), E_α rises from ∼90 to ∼100 kJ mol^{-1}; the second stage is characterized by a decrease in E_α from ∼100 to ∼80 kJ mol^{-1}; the third stage shows an increase in E_α from 80 to 110 kJ mol^{-1}. At $\alpha > 0.1$ both isothermal and nonisothermal E_α-dependencies are quite similar.

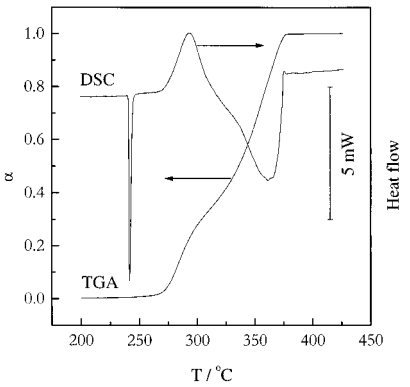

Figure 5. Combined plot of TGA and DSC experiments carried out at a heating rate of 5 °C min^{-1}.

Discussion

DSC and TGA. Analysis of the literature DTA/DSC data[3,22,27,29,30,40−43] suggests (Table 3) that the thermal decomposition of AP usually appears as a sequence of two events (peaks), the first of which is exothermic. The second peak may appear as an exothermic or endothermic event, depending on the experimental conditions. When decomposition occurs under the conditions that retard the escape of reaction gases from the reaction zone (elevated pressures, closed pans, static atmosphere, etc), the second event appears as an exothermic peak. Conversely, under the conditions that facilitate the removal of gaseous products (vacuum, open pans, high flow rates of a carrier gas), the second event appears as an endothermic peak. Therefore, when the second event appears as an exothermic peak, it should rather be ascribed to the secondary reactions of gas-phase products than to the solid-state decomposition of AP.

Obviously the open pan DSC runs most closely reproduce the conditions of TGA experiments. According to the open pan DSC data, the thermal decomposition of AP passes sequentially an exothermic and endothermic stage. By comparing TGA and DSC curves (Figure 5) we can see that the point when decomposition turns into the endothermic stage is correlated with the slowdown ($\alpha = 0.30-0.35$) observed in the TGA experiments. The solid residue formed by this moment is chemically identical to the original AP.[7−10] The significant difference is that the 30−35% decomposed AP has a highly porous structure. For the surface areas of porous AP, Galwey and Jacobs[15] and Chang et al.[44] have respectively reported the values of 1.5 and 47.3 $m^2\ g^{-1}$. While Galwey and Jacobs[15] could not obtain a reliable estimate for the surface area of undecomposed AP, Chang et al.[44] have found it to be 1000 times smaller than that for the 30−35% decomposed AP.

The development of the high surface area favors adsorption of the gaseous decomposition products. Ammonia was found[11] to significantly retard the thermal decomposition of AP. DTA experiments[40] conducted under 4 atm of ammonia showed the complete disappearance of the first exothermic peak that corresponds to the solid-state decomposition of AP and that is observed under the same pressure of an inert gas.[27,40] Surface adsorption of ammonia was proposed[45] to be the reason for the cessation of the LTD observed after decomposing 30−35% of initial AP.

(40) Stone, R. L. *Anal. Chem.* **1960**, *32*, 1582.
(41) Pelly, I. *Isr. J. Chem.* **1975**, *13*, 171.
(42) Kishore, K.; Pai Verneker, V. R.; Pitchaiah, K. *J. Anal. Appl. Pyrol.* **1980**, *2*, 45.
(43) Said, A. A.; Al-Qasmi, R. *Thermochim. Acta* **1996**, *275*, 83.
(44) Chang, F.-M.; Huang, C.-C.; Yeh, T.-F.; Liu, C.-S.; Leu, A.-L. *Propellants, Explosives, Pyrotechnics* **1990**, *15*, 261.
(45) Jacobs, P. W. M.; Russel-Jones, A. *AIAA J.* **1967**, *5*, 829.

Scanning electron microscopy has been used[46] to directly observe the development of the surface area during decomposition. The experiments demonstrated that AP heated to the first exothermic peak (27% of decomposition[46]) is a porous material with the square holes whose shape reflects the crystal structure. Continued heating past the exotherm (41% of decomposition) showed considerable sublimation that was observed as smoothing of the square holes.[46]

On the basis of both literature data and data of our TGA and DSC experiments, the solid-state thermal decomposition of AP involves two major stages. In the DSC experiments, the first stage appears as an exothermic peak that corresponds to the formation of thermodynamically stable products such as Cl_2, HCl, H_2O, O_2, N_2O, and NO.[7−10] In TGA experiments, the completion of this stage is observed either as the cessation (LTD) or as the slowdown (HTD) of the mass loss at ∼30% of decomposition. The second stage appears as an endothermic DSC peak that represents dissociative sublimation of AP to ammonia and perchloric acid. Sublimation and exothermic decomposition are most likely to occur throughout the whole process. Since the sublimation rate is proportional to the surface area, the contribution of sublimation is practically negligible (under ambient pressures) at low extents of conversion, but it increases dramatically during decomposition and ultimately outweighs the exothermic contribution of decomposition.

Kinetics. The previous section was concerned with the qualitative regularities of the thermal decomposition of AP. Here, the process is discussed in quantitative terms of the variation of the effective activation energy with the extent of conversion. As seen in Figure 4, the E_α dependencies derived from the isothermal and nonisothermal TGA experiments are quite similar at $\alpha > 0.1$. Note that some quantitative differences in the respective E_α dependencies are unavoidable, because for technical reasons, isothermal and nonisothermal experiments have to be conducted in different temperature regions.[32,47]

Qualitatively different kinetics are observed at $\alpha < 0.1$. To explain this difference we have to take into account that the isothermal decompositions show an induction period. In solid-state decompositions, the induction period is usually associated with nucleation, i.e., the formation of reaction centers (nuclei).[39] This process is followed by nuclei growth that is observed as an acceleration in the decomposition rate. Depending on the rates of nucleation and nuclei growth, the initial decomposition rate may be limited by either of the two processes. The overall rate of decomposition is determined by the concentration of nuclei. Under nonisothermal conditions, the faster the heating rate is, the higher the temperature corresponding to the same concentration of nuclei is. Our nonisothermal experiments have been performed at the heating rates not faster than 15.5 °C min^{-1}. In isothermal experiments, the preset temperatures were reached in ∼1.5 min. This corresponds to an average heating rate of ∼170 °C min^{-1}. Given such fast heating rates, we may expect the concentration of nuclei at the beginning of decomposition to be markedly smaller in the isothermal experiments than in the nonisothermal experiments. Therefore, the initial rate of decomposition is likely to be limited by nucleation in the isothermal experiments and by nuclei growth in the nonisothermal experiments. Then, the values of E_α at $\alpha \rightarrow 0$ derived from the isothermal and nonisothermal data provide respective estimates for the activation energy of nucleation (∼90 kJ mol^{-1}) and nuclei growth (∼130 kJ mol^{-1}) in the thermal decomposition of AP. These estimates agree well with the data of Jacobs and Ng,[27] who report activation energies around 90 and 120 kJ mol^{-1} for the respective processes of nucleation and growth in AP. Although the situation when the activation energy for nucleation is lower than that for growth is not very frequent, it has been observed for thermal decompositions of other solids such as calcium carbonate hexahydrate,[48] mecrcury oxalate,[49] and copper(II) malonate.[50] Therefore, the ascending E_α dependence for the isothermal decomposition at $\alpha = 0-0.1$ reflects the transition of a rate-limiting step from nucleation to nuclei growth. Further variation in E_α ($\alpha < 0.1$) is quite similar to that observed under the nonisothermal conditions.

The exothermic decomposition ($\alpha = 0-0.3$) gives rise to porous AP. The development of the high surface area favors adsorption of the gaseous decomposition products. As a result, the exothermic decomposition is likely to become controlled by mass-transfer along the solid surface and desorption, which are usually characterized by relatively low activation energies. This seems to be a plausible explanation for the observed decrease in the effective activation energy (nonisothermal data in Figure 5) as α approaches 0.3. However, the initial decomposition is likely to be kinetically controlled. Then, the effective value of E_α at $\alpha \rightarrow 0$ gives us an estimate for the activation energy of the thermal decomposition of AP. This value is ∼130 kJ mol^{-1} for the nonisothermal decomposition, and ∼90 kJ mol^{-1} for the isothermal decomposition. Therefore the E_α dependence observed in the region of $\alpha = 0 - 0.3$ reflects a change from kinetically controlled decomposition to decomposition controlled by a mass transfer process. At $\alpha \rightarrow 0.3$, decomposition is still exothermic but markedly slows down. Therefore, the effective activation energy at $\alpha \cong 0.3$ may give us an upper estimate for the activation energy of the mass transfer process responsible for the removal of gaseous products from porous AP. The more realistic (i.e., smaller) value (∼80 kJ mol^{-1}) is found from the isothermal data.

The results of our kinetic analysis suggest that even the initial (exothermic) decomposition shows multistep kinetics. Nevertheless, in the majority of earlier kinetic analyses, this process was treated as a single-step. For this reason, we cannot directly compare the averaged activation energies (Table 1) with the E_α dependencies found in the present work (Figure 4). Although several workers[3,20,22,26] observed nonlinear Arrhenius depend-

(46) Boggs, T. L.; Kraeulte, K. J. *Combust. Sci. Technol.* **1969**, *1*, 75.
(47) Vyazovkin, S.; Wight, C. A. *Int. Rev. Phys. Chem.* **1998**, *17*, 407.
(48) Bradley, R. S.; Colvin, J.; Hume, J. *R. Soc. Proc. A.* **1932**, *137*, 531.
(49) Prout, E. G.; Tompkins, F. C. *Trans. Faraday Soc.* **1947**, *43*, 148.
(50) Carr, N. J.; Galwey, A. K. *Proc. R. Soc. London A.* **1986**, *404*, 101.

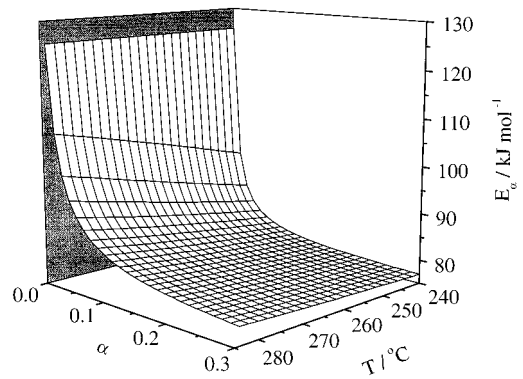

Figure 6. Surface plot of the activation energy estimated from the Manelis−Rubtsov model by varying the extent of conversion and temperature.

encies, only Manelis and Rubtsov[19] proposed a multistep kinetic model for the net process of the solid-state decomposition of AP

$$\frac{d\alpha}{dt} = k_1(1-\alpha)^2 + k_2\alpha(1-\alpha)^2 \qquad (4)$$

We used this empirical model to derive the respective E_α dependence as follows:

$$E_\alpha = -R\left[\frac{d\ \ln\left(\frac{d\alpha}{dt}\right)}{dT^{-1}}\right]_\alpha = \frac{E_1k_1 + E_2k_2\alpha}{k_1 + k_2\alpha} \qquad (5)$$

Substitution of experimentally determined[19] rate constants $k_1 = 10^8 \exp(-15098/T)$ (s^{-1}) and $k_2 = 10^{4.5} \exp(-9109/T)$ (s^{-1}) into eq 5 gives rise to the series of isothermal E_α dependencies depicted as a surface plot in Figure 6. In the experiments conducted by Manelis and Rubtsov, AP decomposed only up to 30%. Therefore, $\alpha = 1$ in their model (eq 4) corresponds to ~30% of AP decomposition (the exothermic process). In our experiments, AP decomposes completely, i.e., $\alpha = 1$ corresponds to 100% of AP decomposition. To make the E_α-dependencies obtained by eq 5 comparable to our data (Figure 4), the α axis (Figure 6) has been properly rescaled after calculations. As we can see in Figure 6, the Manelis-Rubtsov model yields E_α dependencies that are very similar to the dependence we obtained from nonisothermal experiments (Figure 4).

While derived from isothermal data, the activation energies reported by Manelis and Rubtsov do not explicitly account for a lower activation energy in the induction period that we observed for the isothermal decomposition of AP (Figure 4). Perhaps, this short process went unnoticed because Manelis and Rubtsov fit eq 4 to the data related to the full range of the extents of conversion (i.e., $\alpha = 0-1$) without performing a separate fit for the induction period. On the other hand, we cannot rule out that for Manelis and Rubtsov's sample the activation energy of nucleation was close to that for nuclei growth. Because the process of nucleation is extremely sensitive to the prehistory of a solid, the AP samples with different prehistories are likely to show different activation energies for nucleation. For instance, the values of the activation energy of nucleation in orthorhombic AP have been reported to be 155,[27] 210,[51] and 290[52] kJ mol^{-1}. For cubic AP, Jacobs and Ng[27] reported the activation energy for the induction period to vary with the crystal sizes and types of impurities as follows: 92 (large single crystals), 85 (small platelike single crystals), 106 (crystals doped by Ba^{2+}), and 128 (crystals doped by SO_4^{2-}) kJ mol^{-1}.

The development of high surface area plays a crucial role in changing the process from an exothermic to an endothermic regime at $\alpha > 0.3$. The rate of sublimation is directly proportional to the surface area. Then, in accord with the surface area measurements,[44] we may expect that by $\alpha = 0.3$ the sublimation rate increases 1000 times as compared to that at the beginning of decomposition. This appears to be the major reason sublimation ultimately takes over the slow exothermic decomposition controlled by mass-transfer. The exothermic decomposition, however, is most likely to accompany sublimation. Therefore, the progress of the thermal decomposition of AP at $\alpha > 0.3$ is determined by the competition of dissociative sublimation and the exothermic decomposition. The coexistence of these two processes is supported by the fact that the endothermic effect estimated by DSC (140 kJ mol^{-1} after correcting for preceding mass loss) is only about 60% of experimentally found[53] enthalpy of sublimation, 242 ± 8 kJ mol^{-1}.

The activation energy of sublimation (~120 kJ mol^{-1}) was theoretically and experimentally found[23] to be $^1/_2$ of the enthalpy of sublimation. Because this value is greater than that for the mass-transfer processes (~80 kJ mol^{-1}), the relative contribution of sublimation to the overall process rate increases with the temperature. For the nonisothermal data, the variation of the activation energy with temperature can be easily followed by replacing the α values with the respective T_α values related to an average heating rate used for kinetic computations (Figure 4). It is clear from Figure 4 that at $\alpha > 0.3$ the effective activation energy increases with the temperature. The value of E_α corresponding to the maximum temperature represents the greatest contribution of sublimation to the overall rate of decomposition. Consequently, the effective value of E_α at $\alpha \rightarrow 1$ gives us an estimate for the activation energy of sublimation. This value is about 130 kJ mol^{-1} for nonisothermal data.

The E_α dependence derived from the isothermal data (Figure 4) also demonstrates an increase in the effective activation energy in that region. The value of E_α at $\alpha \rightarrow 1$ is 110 kJ mol^{-1}, which is reasonably consistent with the activation energy of sublimation obtained from the nonisothermal data. Overall, the kinetics of the thermal decomposition of AP seems to be quite similar under isothermal and noniosthermal conditions at $\alpha > 0.3$. Both nonisothermal (130 kJ mol^{-1}) and isothermal (110 kJ mol^{-1}) estimates are in accord with the activation energy of sublimation determined by Jacobs and Russel-Jones[23] (125 kJ mol^{-1}).

Table 2 collects the values of the activation energy for the thermal decomposition of AP in a vacuum, i.e.,

(51) Boldyrev, V. V.; Savintsev, Yu. P.; Moolina, T. V. *Proc. 7th Int. Symp. on Reactivity of Solids*; Chapman & Hall: London, 1972; p 421.
(52) Khairetdinov, E. F.; Boldyrev, V. V. *Thermochim. Acta* **1980**, *41*, 63.
(53) Inami, H. S.; Rosser, W. A.; Wise, H. *J. Phys. Chem.* **1963**, *67*, 1077.

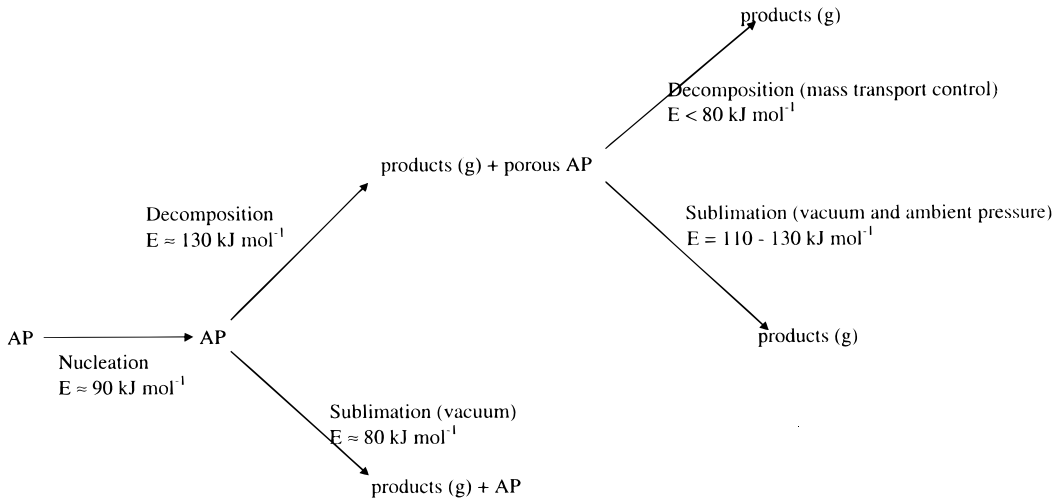

Figure 7. Kinetic scheme of thermal decomposition of cubic AP in the temperature region 250−400 °C.

under conditions when the process is controlled by dissociative sublimation. Analysis of the data from Table 2 suggests that the value obtained by Jacobs and Russel-Jones[23] stands out as being noticeably greater. However, we should take into account that Jacobs and Russel-Jones[23] used in their experiments the residue of LTD (i.e., 30% decomposed porous AP), whereas all other experiments were performed on undecomposed AP. In our experiments, we observe sublimation (endothermic DSC peak) only after 30% of decomposition. Then, our measurements should yield the activation energy of sublimation of the LTD residue and should rather be consistent with the value determined by Jacobs and Russel-Jones.[23] They also found that sublimation of the LTD residue proceeds with the same activation energy under ambient pressures and in a vacuum.

The difference in the values of the activation energy for sublimation of undecomposed AP and of LTD residue may be the evidence that the mechanism of sublimation changes with the development of the high surface area in AP. For undecomposed AP, Aleksandrov and Khairetdinov[54] suggest a stepwise mechanism of sublimation. According to this mechanism, sublimation of the reaction products occurs as a successive diffusion from the most strongly bound state to the least strongly bound state that corresponds to the adsorption on a smooth surface. The proposed model suggests the activation energy to be $^1/_3$ of the enthalpy of sublimation, i.e., ∼80 kJ mol^{-1}, which is consistent with the values reported for sublimation of undecomposed AP (Table 2).

Conclusion

On the basis of our kinetic analysis as well as on the literature data, we can propose a relatively simple kinetic scheme (Figure 7) for the thermal decomposition of cubic AP. The process starts from nucleation that appears as an induction period on isothermal kinetic curves. The activation energy of nucleation is an ambiguous value that depends on the prehistory of an AP sample. As soon as the amount of nuclei reaches the critical mass, thermal decomposition becomes controlled by nuclei growth with the activation energy of about 130 kJ mol^{-1}. At this stage ($\alpha < 0.3$), the overall process, which includes thermal decomposition and quite likely sublimation, is exothermic. The contribution of sublimation is insignificant under ambient pressures. Nevertheless, it increases with decrease of pressure and may become prevailing in a vacuum. The activation energy of sublimation in a vacuum appears to be about 80−90 kJ mol^{-1}. The high surface area of porous AP formed during the exothermic decomposition causes the process to turn into a slow regime controlled by mass transfer with an activation energy less than 80 kJ mol^{-1}. Processes that occur at the late stages ($\alpha > 0.3$) are governed by competition between the mass transfer controlled decomposition and sublimation. In open systems, the latter makes the overall process endothermic. The difference in the activation energy for sublimation of porous and of undecomposed AP is most likely due to the change in the mechanism of sublimation.

Acknowledgment. This research is supported in part by the University of Utah Center for Simulations of Accidental Fires and Explosions, funded by the Department of Energy, Lawrence Livermore Laboratory, under subcontract B341493, and by the Office of Naval Research under contract No. N00014-95-1-1339).

CM9904382

(54) Alexandrov, V. V.; Khairetdinov, E. F. *Kinet. Katal.* **1971**, *12*, 1327.